

Article

***In Situ* Electrochemical Promotion by Sodium of the
Platinum-Catalyzed Reduction of NO by Propene**

Ioannis V. Yentekakis, Alejandra Palermo, Neil C. Filkin, Mintcho S. Tikhov, and Richard M. Lambert

J. Phys. Chem. B, **1997**, 101 (19), 3759-3768 • DOI: 10.1021/jp963052c

Downloaded from <http://pubs.acs.org> on November 26, 2008

More About This Article

Additional resources and features associated with this article are available within the HTML version:

- Supporting Information
- Links to the 1 articles that cite this article, as of the time of this article download
- Access to high resolution figures
- Links to articles and content related to this article
- Copyright permission to reproduce figures and/or text from this article

[View the Full Text HTML](#)



ACS Publications
High quality. High impact.

In Situ Electrochemical Promotion by Sodium of the Platinum-Catalyzed Reduction of NO by Propene

Ioannis V. Yentekakis,[†] Alejandra Palermo,[‡] Neil C. Filkin, Mintcho S. Tikhov, and Richard M. Lambert*

Department of Chemistry, University of Cambridge, Cambridge CB2 1EW, England

Received: October 3, 1996; In Final Form: February 19, 1997[⊗]

The Pt-catalyzed reduction of NO by propene exhibits strong electrochemical promotion by spillover Na supplied from a β'' -alumina solid electrolyte. In the promoted regime, rate increases by an order of magnitude and is achievable. At sufficiently high loadings of Na the system exhibits poisoning, and excursions between the promoted and poisoned regimes are fully reversible. Reaction kinetic data obtained as a function of catalyst potential, temperature, and gas composition indicate that Na increases the strength of NO chemisorption relative to propene. This is accompanied by weakening of the N–O bond, thus facilitating NO dissociation, which is proposed as the critical reaction-initiating step. The dependence of N₂/N₂O selectivity on catalyst potential is in accord with this view: Na pumping to the Pt catalyst favors N₂ production at the expense of N₂O. X-ray photoelectron spectroscopic (XPS) data confirm that electrochemical promotion of the Pt film does indeed involve reversible pumping of Na to or from the solid electrolyte. They also show that under reaction conditions the promoter phase consists of a mixture of sodium nitrite and sodium nitrate and that the promoted and poisoned conditions of the catalyst correspond to low and very high loadings of these sodium compounds. Under all reaction conditions, a substantial fraction of the promoter phase is present as 3D crystallites.

Introduction

Electrochemical promotion (EP), discovered and developed by Vayenas *et al.*, is an entirely new way of controlling catalyst performance.¹ Reference 1 provides a detailed account of the phenomenology and outlines a theoretical basis in terms of which the EP effect may be interpreted. The method entails electrochemical pumping of ions from a solid electrolyte to the surface of a porous, catalytically active metal film: the resulting changes in work function ($\Delta\Phi$) of the catalyst alter the adsorption enthalpies of adsorbed species and the activation energies of reactions involving these species. It has been shown¹ that the electrochemically induced changes in catalyst potential measured with respect to a reference electrode (ΔV_{WR}) are identical to $\Delta\Phi$. The effects on activity and selectivity are reversible, and the phenomenon provides a uniquely efficacious and controllable method for the *in situ* tuning of working catalytic systems. Thus, in addition to its potential practical utility, EP also provides a means for the systematic investigation of certain aspects of promoter action in a manner that was hitherto not possible. Note that EP is strongly non-faradaic: one is not dealing with conventional electrocatalysis. The electrochemically induced catalytic rate changes are typically 10^3 – 10^5 times greater than the rate of supply of promoter species. The EP phenomenon has been reported for over 40 catalytic reactions on Pt, Rh, Pd, Ag, Ni and IrO₂ catalyst films with a variety of solid electrolytes including oxygen,^{2–4} sodium,^{1,5–8} fluorine,⁹ and hydrogen ion conductors.¹⁰

It is well-known that reactions involving the catalytic reduction of NO are of major environmental importance.¹¹ In

this connection, Rh plays a key role in current three-way converters because it is highly effective for the dissociative chemisorption and reduction of NO. In a recent study of electrochemical promotion of the CO + NO reaction over Pt,⁸ we showed that the selectivity, and especially the activity, of a Pt film electrochemically fed with sodium from a β'' -alumina (a Na⁺ ion conductor) support could be dramatically enhanced: in effect, Pt could be induced to behave like Rh. The results indicated that Na induces NO dissociation which is thought to be the crucial reaction-initiating step. Here we present an extension of this work to a potentially more important system: EP of the reduction of NO by propene over Pt/ β'' -alumina. (Propene is the major constituent of the hydrocarbon component in automotive exhaust and is the industry standard for catalyst testing.) Very large rate accelerations and substantial gains in selectivity towards N₂ production were achieved, while XP spectra gave insight into the nature of the promoting species and the origin of the poisoning effects observed at high promoter loadings.

Methods

The platinum catalyst (working electrode, W) consisted of a porous continuous thin film (~ 2 cm² geometric area) deposited on one face of a 20 mm diameter β'' -Al₂O₃ disc (Ceramatec) as described in detail elsewhere.⁵ Au reference (R) and counter (C) electrodes were attached to the other face of the solid electrolyte wafer (see Figure 1, ref⁵) by vacuum evaporation, a procedure that produced electrodes with good adhesion and low electrical resistance. The actual active surface area of the Pt catalyst electrode (W) was estimated by comparing the observed rate of CO oxidation under standard conditions (6 kPa of O₂, 1.8 kPa of CO, 623 K, and $V_{WR} = +800$ mV) with those obtained⁵ using samples whose surface area had been directly determined using an O₂/CO titration technique.¹² This gave a value of 5×10^{-7} mol of Pt (~ 200 cm²) for the active metal area. The Pt/ β'' -Al₂O₃/Au sample was suspended in a quartz,

* Corresponding author. Telephone 44 1223 336467; FAX 44 1223 336362; e-mail rml1@cam.ac.uk.

[†] Institute of Chemical Engineering and High Temperature Chemical Processes and Department of Chemical Engineering, University of Patras, Patras, GR-26500, Greece.

[‡] Institute of Materials Science and Technology (INTEMA), UNMDP-CONICET, J. B. Justo 4302, (7600) Mar del Plata, Argentina.

[⊗] Abstract published in *Advance ACS Abstracts*, April 1, 1997.

atmospheric-pressure well-mixed reactor with all three electrodes exposed to the reactant gas mixture.^{7,8} The reactor volume was 115 cm³, and the system behaved as a single pellet, continuous stirred tank reactor (CSTR) as described and discussed elsewhere.^{4,5,7,13,14}

Inlet and exit gas analysis was carried out by a combination of on-line gas chromatography (Shimadzu-14B; molecular sieve 5A and Porapak-N columns) and on-line mass spectrometry (Balzers QMG 064). N₂, N₂O, CO, CO₂, and C₃H₆ were measured by gas chromatography, and NO was measured continuously by mass spectrometry after performing the required calibrations. The mass spectrometer was also used to monitor continuously $m/z = 28$ (N₂ + CO), 44 (CO₂ + N₂O), 16 (O), 41 (propene), and 17 (NH₃). Reactants were pure NO (Distillers MG) and propene (Matheson) diluted in ultrapure He (99.996%) and fed to the reactor by mass-flow controllers (Brooks 5850 TR). The total flow rate was kept essentially constant in all experiments at 1.3×10^{-4} mol s⁻¹ (190 cm³ (STP)/min), with partial pressures P_{NO} , and $P_{\text{C}_3\text{H}_6}$ varying between 0–6.5 and 0–0.4 kPa, respectively. Conversion of the reactants was restricted to <15% in order to avoid mass transfer limitations.

An AMEL 553 galvanostat–potentiostat was used to carry out measurements in both galvanostatic and potentiostatic modes. In the galvanostatic mode, constant current, I , was applied between the catalyst (W) and the counter electrode (C) while monitoring the potential V_{WR} between the catalyst and the reference electrode (R).⁸ This gave information about the time-dependent behavior of the system. The galvanostatic transient behavior of V_{WR} was also used to calibrate the Na coverage scale.^{5,15} As noted above, changes in catalyst potential, V_{WR} , are related to concomitant changes in catalyst work function according to $e\Delta V_{\text{WR}} = \Delta(e\Phi)$ as predicted theoretically¹ and confirmed experimentally.¹⁶

In the potentiostatic mode, a constant potential V_{WR} was maintained between the catalyst and the reference electrode—this gave information about activity, selectivity, and kinetics under steady-state conditions. Most experiments were carried out in the potentiostatic mode by following the effect of the applied catalyst potential (V_{WR}) on reaction rates. Periodic reversal of the direction of Na⁺ pumping (required in order to regenerate a clean Pt surface on the working electrode) appeared to avoid possible difficulties due to Na depletion of the electrolyte. In this connection, note that an amount of sodium equivalent to $\theta_{\text{Na}} \sim 3$ corresponds to 0.04% of the total amount of Na in the electrolyte wafer.

XPS measurements were carried out in a VG ADES 400 ultrahigh-vacuum spectrometer system. The EP sample was mounted on a machinable ceramic block resistively heated by embedded, electrically insulated tungsten filaments. XP spectra were acquired with Mg K α radiation with the Pt catalyst electrode always at ground potential; appropriate electrochemical potentials (V_{WC}) were imposed between the Pt working electrode and the Au counter electrode by applying voltage bias to the latter. The potential (V_{WR}) of the Pt working electrode with respect to the Au reference electrode was also monitored. Quoted binding energies are referred to the Au 4f_{7/2} emission at 83.8 eV, and Au reference spectra were provided by the Au wire which formed the electrical connection to the working electrode. The EP catalyst assembly used for XPS study measurements was first tested in the EP reactor to ensure that it exhibited the same catalytic behavior as the samples used to acquire the reactor data.

Results

The only detectable reaction products were CO₂, N₂, N₂O and H₂O. Overall carbon and nitrogen mass balance closures

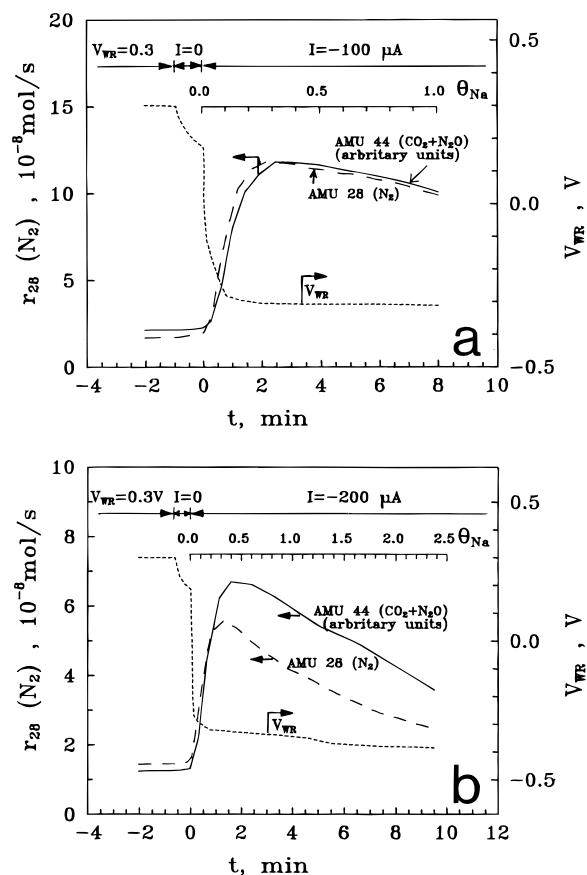
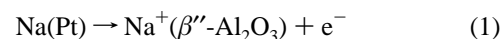


Figure 1. Galvanostatic transients. Showing response of mass 44 rate (N₂O + CO₂) (solid line), N₂ rate (broken line), and catalyst potential (dotted line), in response to a step change in constant applied current. Conditions: (a) inlet partial pressures $P_{\text{NO}}^0 = 1.3$ kPa, $P_{\text{C}_3\text{H}_6}^0 = 0.6$ kPa, $T = 648$ K; (b) $P_{\text{NO}}^0 = 0.8$ kPa, $P_{\text{C}_3\text{H}_6}^0 = 0.4$ kPa, $T = 648$ K.

within 5% were found by a combination of GC and mass spectroscopic analyses.

Transient Electrochemical Promotion. In order to obtain an estimate of the Na coverage corresponding to any given value of V_{WR} , galvanostatic transients were obtained and analyzed as described previously by Vayenas *et al.*¹⁵ Such transients also provide a useful means of rapidly mapping out the dependence of reaction rates on Na coverage in advance of the much more detailed and laborious steady-state measurements.

Figure 1a shows a typical galvanostatic transient: it depicts the effect of applying a constant negative current (Na supply to the catalyst) on the catalyst potential, V_{WR} , and on the $m/z = 28$ (N₂) and 44 (CO₂ + N₂O) signals. The experimental procedure was as follows: first ($t \leq 0$), the surface was electrochemically cleaned of Na by application of a positive potential (V_{WR}) of the order of 300 mV until the current between the catalyst and counter electrode vanished. This current corresponds to the reaction



The potentiostat was then disconnected ($I = 0$ at $t = -1$ min) and V_{WR} relaxed to the value imposed by the gaseous composition. Subsequently, the galvanostat was used to impose a constant cathodic current $I = -100 \mu\text{A}$ at $t = 0$, thus pumping Na to the catalyst surface at a rate $I/F = 1.04 \times 10^{-9}$ mol of Na/s. In order to construct an abscissa corresponding to the Na coverage on the Pt surface (θ_{Na} , see Figure 1), θ_{Na} was computed from Faraday's law according to

$$\frac{d\theta_{\text{Na}}}{dt} = \frac{-I}{FN} \quad (2)$$

where $N (=5.0 \times 10^{-7} \text{ mol})$ is the number of available Pt sites independently measured as described above. Under these conditions (Na pumping to the catalyst surface), a pronounced decrease in the catalyst potential V_{WR} , and consequently in the catalyst work function ($e\Delta V_{\text{WR}} = \Delta e\Phi$) occurred. This was accompanied by a very marked increase (by a factor of 7) in the production rate of N_2 . As is apparent from Figure 1, the reaction rates (r) exhibit maxima for $\theta_{\text{Na}} \sim 0.3\text{--}0.4$ at $V_{\text{WR}} \sim -300 \text{ mV}$, and continued Na pumping eventually leads to poisoning of the system. The $m/z = 44$ ($\text{CO}_2 + \text{N}_2\text{O}$) signal is given in arbitrary units because the separate contributions of CO_2 and N_2O could not be measured by mass spectrometry alone. Potentiostatic imposition of the initial V_{WR} restored the rates to their initial unpromoted values, corresponding to clean Pt, thus demonstrating that the system was perfectly reversible.

In general, the relationship between V_{WR} and θ_{Na} depends on the gaseous composition as discussed previously.^{5,8} For present purposes, it is sufficient to note that the $V_{\text{WR}}/\theta_{\text{Na}}$ calibration (Figure 1a) was performed in the identical gas atmosphere to that used in the steady-state measurements to be described below. Figure 1b shows a transient obtained using the same reactant partial pressure ratio as that in Figure 1a, but with a higher current and smaller reactant pressures. In line with expectation the maximum is more pronounced in this case, and it is interesting to note that it occurs at essentially the same value of θ_{Na} as that found in Figure 1a.

It should be emphasized that the " θ_{Na} " scales in Figure 1a,b are computed on the basis of uniform coverage of the entire Pt surface by the relevant amount of electrochemically supplied Na. That is, " θ_{Na} " is proportional to the total amount of pumped Na. If the morphology of the promoter phase is nonuniform, e.g., 3D islands of Na compound(s) coexisting with a submonolayer film of promoter species on the Pt surface, $\theta_{\text{Na}} > 1$ would still correspond to a catalytically active system. The data in Figure 1a,b suggest that this is indeed the case—nominal coverages of greater than unity exhibit activity well in excess of clean Pt because a substantial amount of the promoter material is present as 3D crystallites. XPS data (see below) are in accord with this view. A useful check is provided by ΔV_{WR} transients measured in He as opposed to the reaction gas. These show monotonic behavior similar to that shown in Figures 1a,b. Additionally, the behavior of $\Delta V_{\text{WR}} (= \Delta\Phi)$ as a function of computed θ_{Na} is in good quantitative agreement with results obtained for Pt{111}/Na in ultrahigh vacuum.¹⁷ This indicates that in a He atmosphere one is dealing with metallic Na uniformly distributed on the Pt surface.

A convenient parameter for expressing electrochemically induced promoting or poisoning effects is the promotion index, P_{Na} , defined¹⁸ as

$$P_{\text{Na}} = (\Delta r/r_0)/\Delta\theta_{\text{Na}} \quad (3)$$

This takes positive or negative values for promotion or poisoning, respectively. Here, P_{Na} values up to 20 were found for the rate of N_2 production in the promoted regime. This is followed by a poisoned regime for $\theta_{\text{Na}} > 0.5$. This "volcano type" behavior is also apparent in the potentiostatic, steady-state data to be presented in the following section. Similar promoting—poisoning behavior of Na has been also observed in the cases of CO^5 and ethylene¹³ oxidation and NO reduction by CO^8 over Pt/ β'' -alumina under appropriate conditions.

Steady-State Effect of Catalyst Potential (V_{WR}) on Reaction Rates. Parts a, b, and c of Figure 2 show steady-state rate

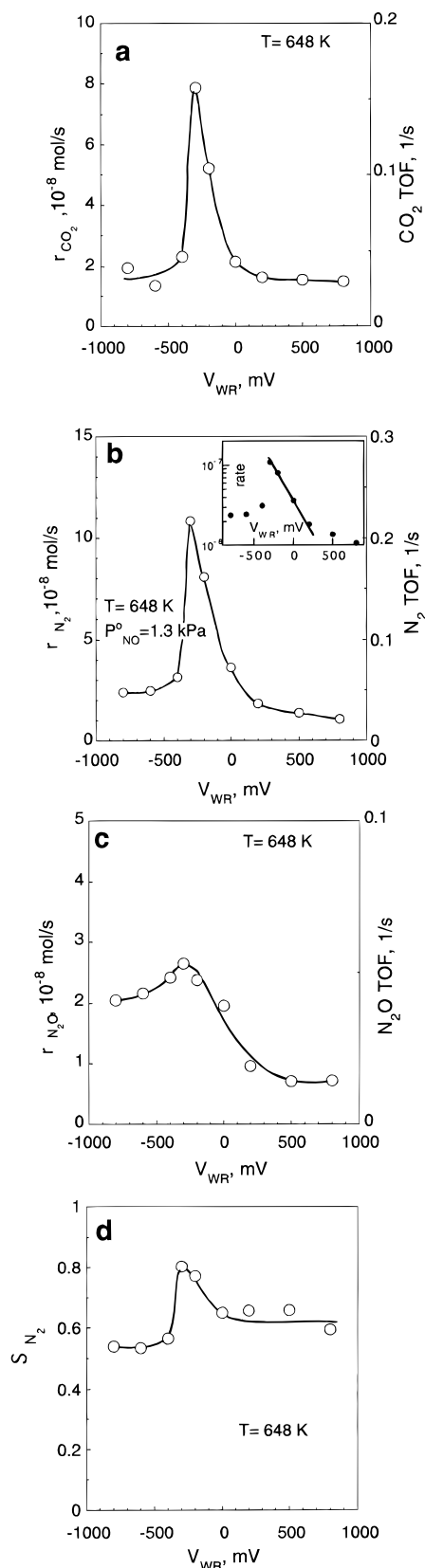


Figure 2. Effect of catalyst potential, V_{WR} on (a) CO_2 , (b) N_2 , (c) N_2O production rates and on N_2 selectivity (d). Conditions: $P_{\text{C}_3\text{H}_6}^0 = 0.6 \text{ kPa}$; $P_{\text{NO}}^0 = 1.3 \text{ kPa}$, $T = 648 \text{ K}$, total flow rate $F_t = 1.7 \times 10^{-4} \text{ mol/s}$.

data for CO_2 , N_2 , and N_2O production as a function of V_{WR} at 648 K for constant inlet pressures (P_{NO}^0 , $P_{\text{C}_3\text{H}_6}^0$) of NO and C_3H_6 .

Figure 2d depicts the V_{WR} dependence of the selectivity toward N_2 where the latter quantity is defined as

$$S_{N_2} = r_{N_2} / (r_{N_2} + r_{N_2O}) \quad (4)$$

The data presented in Figure 2a,b show that, for both the CO₂ and N₂ rates, a regime of strong promotion is followed by strong poisoning. Relatively low rates are observed at both very positive (clean Pt) and very negative (high Na loading) catalyst potentials. In particular, both rates exhibit an exponential increase with decreasing V_{WR} in the interval ~ 0 to -300 mV: this is made more apparent by a logarithmic plot, e.g., as shown in the inset to Figure 2b. The rate of N₂O production also exhibits “volcano-type” behavior, though the effect is not as pronounced (Figure 2c)—the point is of significance with respect to our subsequent discussion of the reaction mechanism. The maximum enhancements in CO₂, and N₂ rates over the clean surface rates are ~ 7 , and for N₂O ~ 3 . Note also that the selectivity toward N₂ increases from 60% on the clean Pt surface to 80% on the Na-promoted Pt surface at $V_{WR} \sim -300$ mV.

Control experiments were carried out in which the total flow rate was varied by a factor of 2 in order to verify that the observed changes in activity were due to a true increase in surface reaction rates and not due to mass transfer limitations in the reactor. As found in previous EP studies with Pt/ β'' -alumina^{5,13} for any given reaction conditions, the promotional effect is entirely controlled by the applied potential and the resulting Na coverage. After current interruption the promoted rates remained practically constant over periods of many minutes—the slow decline that occurred under open circuit conditions is associated with various possible loss mechanisms for the surface Na species, e.g., slow evaporation at reaction temperature. In order to restore the initial unpromoted catalytic rate, potentiostatic imposition of the initial potential of $+300$ mV was necessary.⁵ It is significant that in a reaction gas environment the total amount of Na pumped in order to attain a given value of V_{WR} was about an order of magnitude higher than in a He environment. This is consistent with the accumulation of the Na into 3D islands of a surface compound in the presence of a reactive atmosphere.

Effect of $P_{C_3H_6}$ and P_{NO} on Promoted and Unpromoted Steady-State Rates. Parts a, b, and c of Figure 3 show 648 K potentiostatic data for the rates and turnover frequencies (TOFs) of CO₂, N₂, and N₂O taken at four different fixed values of catalyst potential as a function of the outlet pressure of propene, for a fixed NO outlet pressure of 1.4 kPa. Figure 3d shows the corresponding results for the N₂ selectivity, S_{N_2} . In every case the system was perfectly reversible and exhibited no hysteresis when switching between negative and positive catalyst potentials.

The observed rate variations show that the reaction obeys Langmuir–Hinshelwood (LH) type kinetics with the characteristic rate maximum reflecting competitive adsorption of the two reactants. It is also apparent that as the catalyst potential is decreased to more negative values (increasing θ_{Na}), there is a systematic shift of the rate maxima to *higher* propene partial pressure ($P_{C_3H_6}^*$). Figure 4a–d depicts analogous results for the effect of NO at four different catalyst potentials for fixed $P_{C_3H_6} = 0.27$ kPa. The CO₂ and N₂ rates show essentially similar behavior as P_{NO} is varied—a pronounced enhancement in catalytic activity occurs upon decreasing the catalyst potential from 300 to -300 mV. In this case the rate maxima are inaccessible within the constraints imposed by our experimental conditions—here, one expects the opposite effect, namely that increasing levels of Na should shift the (inaccessible) value of P_{NO}^* to *lower* values. A comparison of the trends shown in Figures 3 and 4 indicates that under these conditions the adsorption of propene on Pt is stronger than that of NO.

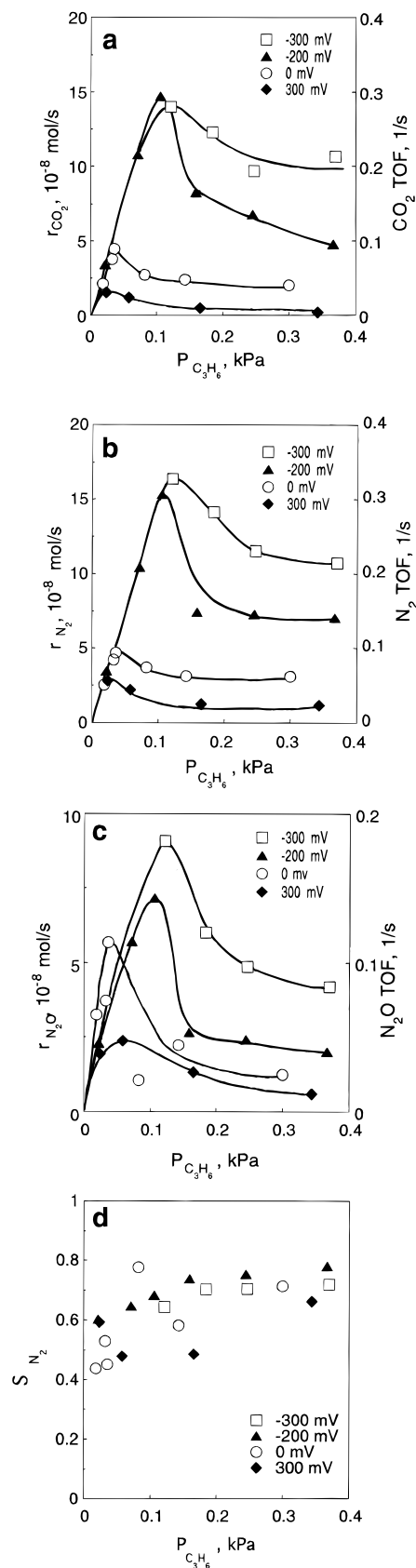


Figure 3. Effect of C₃H₆ partial pressure ($P_{C_3H_6}$) on the rate of (a) CO₂, (b) N₂, (c) N₂O production and on N₂ selectivity S_{N_2} , (d) at different catalyst potentials, V_{WR} . Conditions: $P_{NO} = 1.4$ kPa, $T = 648$ K, total flow rate $F_t = 1.3 \times 10^{-4}$ mol/s.

Effect of Temperature on Promoted and Unpromoted Steady-State Rates. It is of interest to compare the temperature dependent-behavior of the chemically complex NO + propene system with the simpler NO + CO system and the even simpler

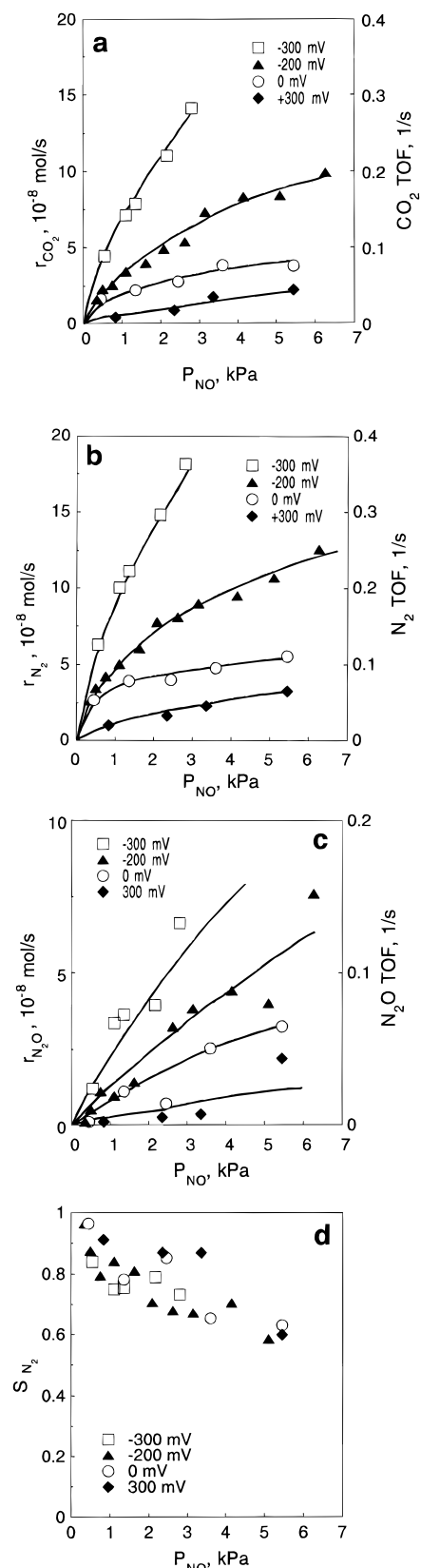


Figure 4. Effect of NO partial pressure (P_{NO}) on the rate of (a) CO_2 , (b) N_2 , (c) N_2O production and on N_2 selectivity S_{N_2} (d) at different catalyst potentials V_{WR} . Conditions: $P_{\text{C}_3\text{H}_6} = 0.27$ kPa, $T = 648$ K, total flow rate, $F_t = 1.3 \times 10^{-4}$ mol/s.

$\text{O}_2 + \text{CO}$ system, the latter two having also been studied under EP conditions over Pt/ β'' -alumina. Accordingly, Figure 5 shows data extracted from Arrhenius plots over the temperature interval 600–675 K for the CO_2 , N_2 , and N_2O production rates as a function of catalyst potential. Although there is some scatter

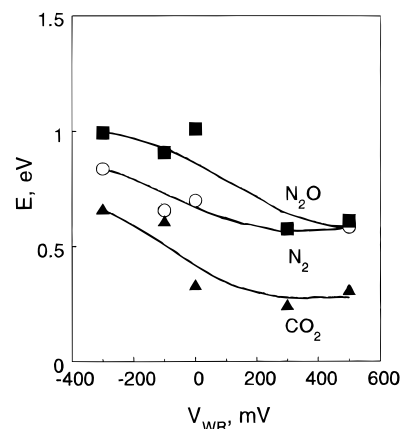


Figure 5. Effect of catalyst potential on the apparent activation energy for (a) CO_2 , (b) N_2 , and (c) N_2O production.

in the data, two features are apparent: (i) the activation energy of all the three reactions increases on going from high positive to high negative potential values; (ii) the activation energy associated with the promoted reaction regime increases monotonically with the Na loading. However, the variation in activation energy with increasing Na coverage is neither abrupt nor pronounced as it is in the case of the EP $\text{CO} + \text{O}_2$ and EP $\text{CO} + \text{NO}$ systems.

XPS Studies of the EP Catalyst. XP spectra were obtained in order to shed light on several important issues. (i) What evidence is there for the reversible transport of Na between electrolyte and catalyst under vacuum conditions? (ii) Does the chemical species transported differ in behavior from vacuum-deposited Na? (iii) What surface species are formed by Na pumping to Pt at reaction temperature and in the presence of the relevant partial pressures of the reactant gases? (iv) What differences are there between the promoted and poisoned regimes? (v) What is temperature stability of the promoter phase?

Figure 6A shows Na 1s spectra acquired at 600 K in ultrahigh vacuum (UHV). The electrochemically cleaned surface ($V_{\text{WR}} = +500$ mV) exhibits a feature at 1074 eV BE which is due to Na in the β'' -alumina visible through cracks in the porous Pt film; this is confirmed by the corresponding O 1s spectra, and similar spectra have been reported for electrochemically cleaned Pt films on yttria-stabilized zirconia.¹⁹ At $V_{\text{WR}} = -600$ mV, two features are now present, that at 1073.5 eV being due to Na pumped to the Pt surface. Note that the β'' -alumina-derived peak has shifted to ~ 1075.5 eV, i.e., by an amount about equal to the change in V_{WR} (1.1 eV). In measurements such as these, one expects $\Delta(\text{apparent BE of Na in electrolyte}) = \Delta V_{\text{WR}}$, because the latter is the change in overpotential between the electrolyte and the electrode due to the electrochemical double layer. The Pt film is at ground potential, and Na 1s photoemission from the Pt should of course appear at fixed kinetic energy, independent of V_{WR} . Thus, our XP spectra clearly reveal the location of and relationship between the two types of Na sampled by photoemission. For intermediate values of V_{WR} the amount of Na on Pt varies monotonically with catalyst potential, and the (constant intensity) Na 1s emission from the β'' -alumina shifts with V_{WR} . This spectral behavior was reproducible and reversible as a function of V_{WR} .

Figure 6B demonstrates that, under UHV conditions, electropumped Na is identical in behavior and in chemical state with Na supplied by vacuum deposition from a Na evaporation source. Control experiments carried out with a Pt{111} sample in the same UHV chamber indicated that the amount of Na deposited on the catalyst film at 300 K was approximately 10^{15}

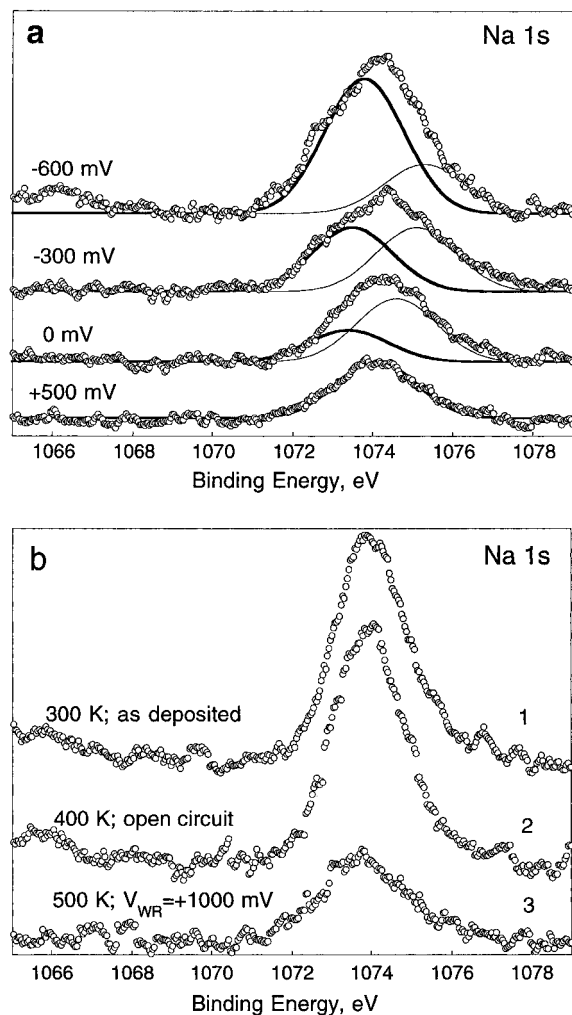


Figure 6. Na 1s XPS. (a) Showing effect of catalyst potential in pumping sodium to/from the Pt film under UHV conditions at 600 K. (b). Demonstrating electrochemical pumping of vacuum-deposited Na away from the surface under UHV conditions at sufficiently high temperature and positive catalyst potential.

cm^{-2} (spectrum 1). Heating to 400 K under open circuit conditions caused no change (spectrum 2). At 500 K (when the β'' -alumina becomes appreciably conducting) and with $V_{\text{WR}} = +1000$ mV, the vacuum-deposited Na was strongly pumped away from the surface (spectrum 3).

The XP spectra in Figure 7 were obtained after exposing the appropriately biased catalyst film to the *conditions of temperature and reactant partial pressures typical of those encountered in the reactor* ($P_{\text{C}_3\text{H}_6} = 0.6$ kPa, $P_{\text{NO}} = 1.2$ kPa, $T = 600$ K). During exposure of the catalyst to the reaction mixture, the V_{WR} conditions were such that the Pt film was either (i) electrochemically clean, (ii) promoted, or (iii) poisoned. The spectra were acquired after a pump-down period of 2 h. The sample temperature was lowered to 420 K before pump-down, and the imposed voltage bias (V_{wc}) was switched off when the sample temperature was below 450 K, i.e., when the Na mobility was low. It is apparent from the N 1s spectra (Figure 7A) that no detectable N-containing species were retained on either the clean or the promoted Pt film. However, the poisoned film shows a very significant line at 405.6 eV, which we ascribe²⁰ to sodium nitrite (NaNO_2). Note in the figure that exposure of this surface to the base vacuum for 10 h at 420 K resulted in removal of the nitrite, presumably due to slow reaction with ambient reducing gases. Figure 7B (upper) shows corresponding (raw) Na 1s data from which it is clear that the loading of Na compounds is highest on the poisoned surface and smallest on

the electrochemically cleaned surface, with the promoted surface level lying in between. Figure 7c shows the corresponding Na *KLL* X-ray-excited Auger spectra—notice that the difference in integrated intensities between the promoted and poisoned cases is much more apparent here. It is important to note that the absolute intensity of the Pt 4f spectrum was measurably attenuated on both the promoted and poisoned surfaces relative to the electrochemically cleaned case (~ 6 and $\sim 15\%$, respectively), indicating a substantially higher loading of Na surface compounds in the latter case. Based on our Pt{111}/Na calibration, the estimated Na loadings of the promoted and poisoned surfaces are $\geq 1.5 \times 10^{15}$ and $\geq 4.5 \times 10^{15}$ cm^{-2} , i.e., equivalent to $\theta_{\text{Na}} \geq 1$ and ≥ 3 , respectively. The former value again implies that even in the promoted case, a substantial proportion of the Na compound(s) must be present in 3D islands, thus leaving a significant amount of uncovered (promoted) Pt surface on which the reaction takes place. That is, one has Volmer–Weber growth of the promoter on the metal surface: the driving force behind agglomeration comes partly from the 3D Madelung energy of the polar crystals that are formed.

Analogous C 1s spectra are shown in Figure 7d: carbon-containing species are detectable only on the clean and promoted surfaces. Finally, Figure 7e shows O 1s results. The behavior is similar to that of the N 1s spectra: the promoted surface shows no detectable lines; the poisoned surface shows peaks at 531 and 535 eV BE, and these are quenched by 10 h exposure to the ambient vacuum at 300 K.

As will be argued below, the data in Figure 7 are to varying extents influenced by the sample handling procedure and especially by continuing reactions that occurred during reactor pump-out and sample cool-down, prior to transfer into the spectrometer. In order to characterize the promoter/poison phase(s), their temperature stability and their reactivity in more detail, XP spectra were also acquired after *sequential* exposure of the sample to NO followed by propene. The results of this approach are illustrated in Figure 8. The spectra in Figure 8a were acquired as a function of temperature under open circuit conditions after gas pump-out. The spectra in Figure 8b,c were acquired as a function of gas exposure at 485 K under open circuit conditions; data were recorded at 485 K, also under open circuit conditions, so as to avoid any voltage/temperature-assisted effects. The object of this procedure was to “freeze out” the catalyst surface in a condition that captured at least some aspects of its properties under actual EP reaction conditions. Figure 8a shows temperature-dependent effects, as follows. NO dosing at 600 K leads to the formation of two distinct sodium nitroxy surface compounds. The 405 eV BE is assigned to NaNO_2 (as above in regard to Figure 7A); the 409 eV BE is assigned to NaNO_3 .²¹ Heating to 500 K leads to a definite ($\sim 25\%$) increase in intensity of the nitrite emission while the nitrate emission is constant within experimental error. We attribute this to increased dispersion of the nitrite but not the nitrate (consistent with the melting points of the bulk compounds: 544 and 580 K respectively). After 520 K heating the nitrite begins to diminish relative to the nitrate, and after 530 K heating the nitrite intensity is the smaller of the two—again, consistent with the decomposition temperatures of the bulk compounds (590 and 650 K).

Discussion

As noted above, the term “Na coverage” does not imply that the promoter is thought to be present in the form of chemisorbed metallic sodium, as it would be in vacuum.

In the reaction mixture one expects the formation of surface compounds of Na—in the present case, carbonate and nitrate

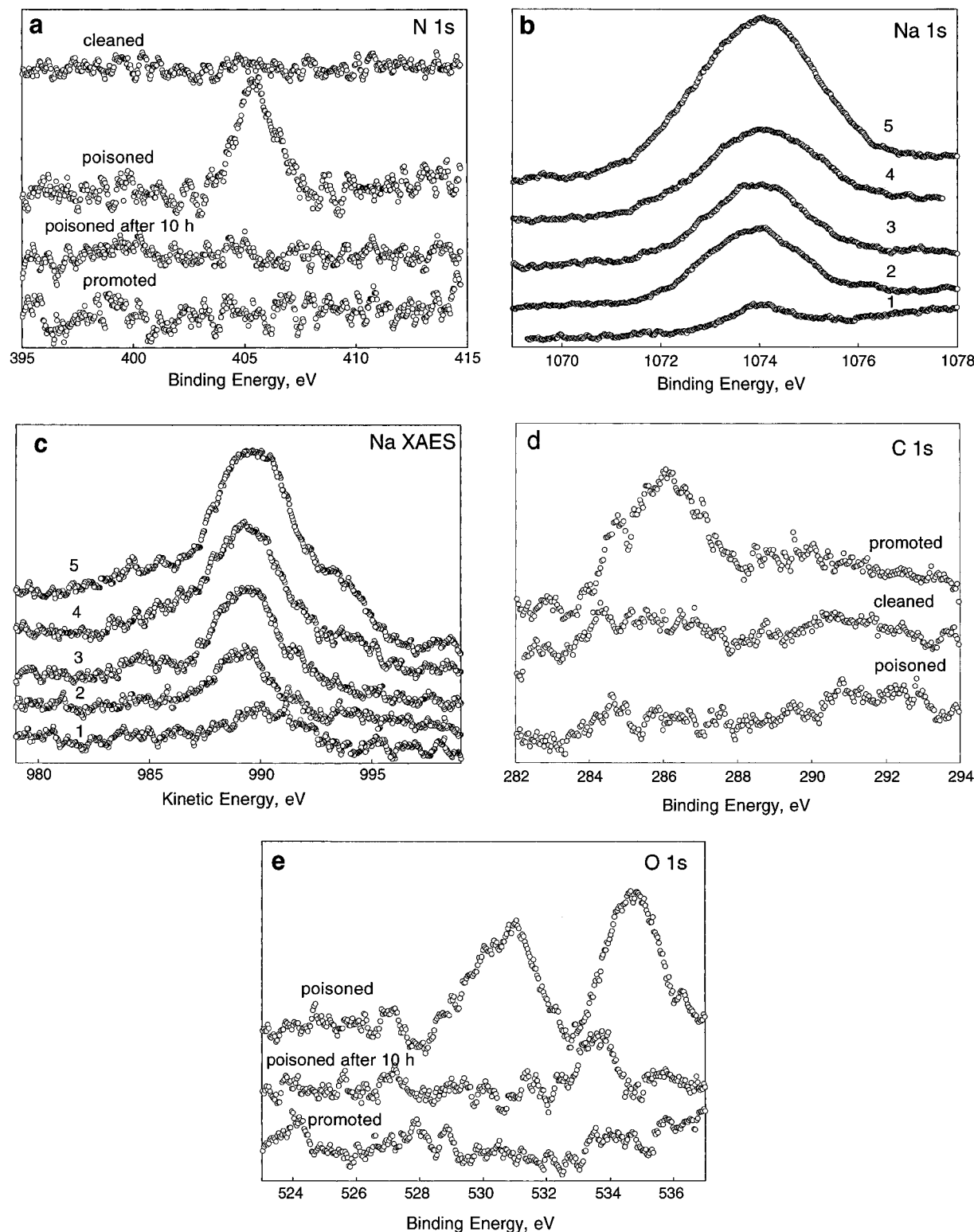


Figure 7. XP spectra of catalyst film after exposure to reaction mixture for 15 min ($P_{\text{C}_3\text{H}_6} = 0.6$ kPa, $P_{\text{NO}} = 1.2$ kPa, $T = 600$ K). The results refer to electrochemically cleaned, promoted, and poisoned conditions. (a) N 1s. (b) Na 1s. 1, +600 mV; 2, -250 mV; 3, -250 mV, after exposure to reaction mixture; 4, -500 mV; 5, -500 mV, after exposure to reaction mixture. (c) Na KLL XAES. 1-5, same conditions as (b). (d) C 1s. (e) O 1s. (a) and (e) also show the effect of continued reaction with ambient.

are plausible possibilities; the XP spectra provide relevant information. For present purposes, we note that adsorbed polar alkali compounds lead to large decreases in work function relative to the clean metal which are of the same order as those produced by the pure alkali metal itself. Substantial changes in catalyst potential are therefore still to be expected under electropumping in a reactive atmosphere.

NO reduction by propene exhibits strong electrochemical

promotion under Na pumping to the catalyst (Figure 2). As discussed below and suggested earlier⁸ in connection with our earlier work on EP of the CO + NO reaction, we infer that the promotional effect is due to *enhanced NO chemisorption and dissociation on the Pt surface* induced by electrochemically pumped Na. Recall that the polycrystalline Pt film consists mainly of large crystallites ($\sim 1 \mu\text{m}$) whose external surfaces are dominated by low index planes: such low index planes of

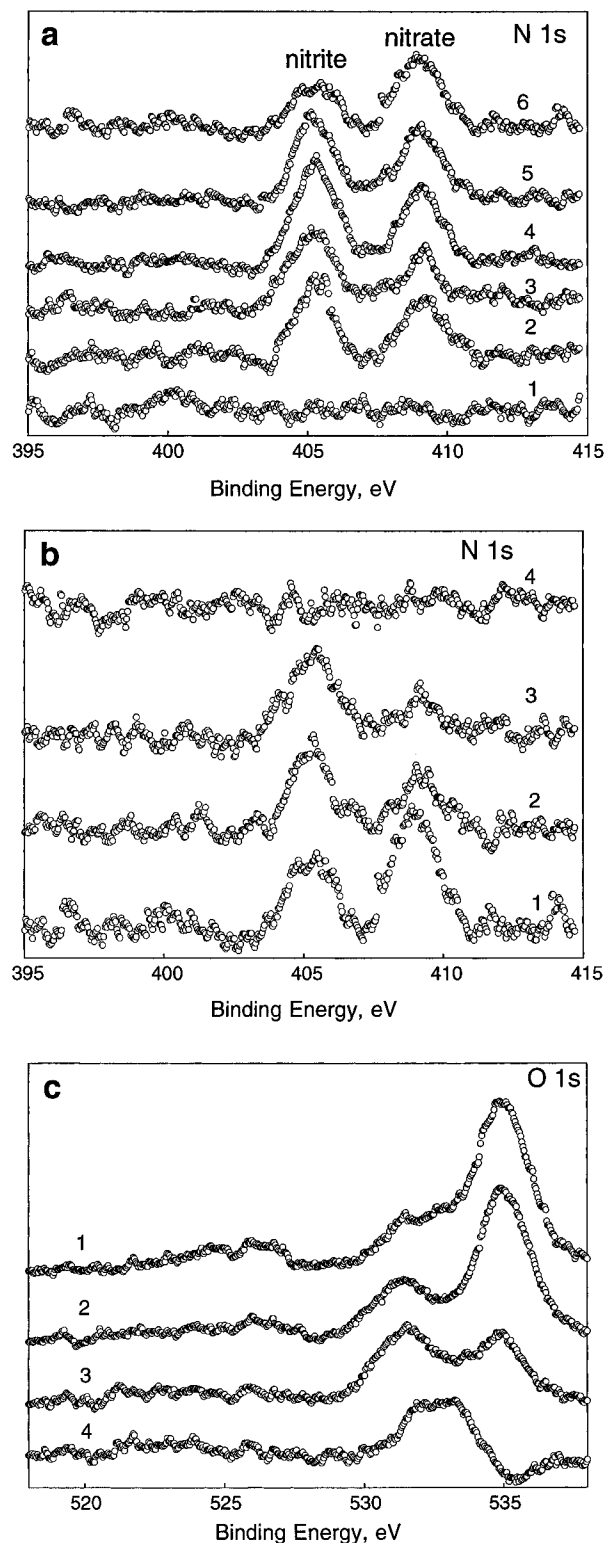


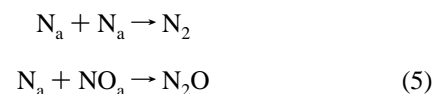
Figure 8. N 1s spectra (open circuit) after exposure to NO at 600 K and -500 mV, showing the effect of (a) temperature: 1, clean, 600 K; 2, 470 K; 3, 485 K; 4, 510 K; 5, 530 K; 6, 560 K. (b) differential reactivity of nitrate and nitrite species toward propene dosed at 485 K: 1, as 6 in (a); 2, 10^3 langmuirs; 3, 6×10^3 langmuirs; 4, 3×10^6 langmuirs; (c) O 1s spectra corresponding to (b).

Pt are known to be relatively ineffective for NO dissociation.²² Na-induced NO dissociation produces the O_a species which are then responsible for initiating the ensuing oxidation reactions of adsorbed propene and propene fragments. The maximum gains in rate over the clean surface rates are of the order of factors of 13 and 25 for N_2 and CO_2 production, respectively (Figures 3 and 4). In the region of strong electrochemical

promotion (0 to -350 mV), the activity toward formation of all products shows an exponential increase with (decreasing) catalyst potential, as predicted by the model of Vayenas.^{1,3} Eventually, at around -350 mV, there is a precipitous fall in rates as the amount of Na species increases beyond a critical value; i.e., the regime of electrochemical promotion is followed by a regime of strong poisoning. This poisoning behavior is discussed below.

The dependence of activity and selectivity on catalyst potential may be rationalized by considering the effects of the Na promoter species on the surface chemistry of propene and NO. At high positive V_{WR} the Pt surface is free of sodium and covered mainly with propene: the relative strengths of propene and NO chemisorption on Pt are apparent from Figures 3 and 4. We postulate that the low clean surface residual rate is due to dissociation of NO at defect sites; as noted above, we take the view that $NO_a \rightarrow N_a + O_a$ is the reaction-initiating step.

As the catalyst potential is decreased toward negative V_{WR} values (pumping Na to the Pt), the electronic effect of the sodium promoter strengthens the Pt–N bond (increasing NO coverage) and weakens the N–O bond (facilitating NO dissociation). The dissociation of chemisorbed diatomic molecules in the field of coadsorbed cations has been discussed in detail by Lang *et al.*²³ More recently, the Na-induced dissociation of NO on Pt{111} has been demonstrated directly.²⁴ Thus, the effect of the promoter is to activate previously inactive crystal planes on the catalyst surface toward NO dissociation. This effect increases progressively with the amount of Na pumped, and the exponential dependence of rate on V_{WR} in the promoted regime suggests that changes in catalyst work function are indeed strongly correlated with the dramatically increased activity.¹ In addition, Na pumping also enhances the selectivity toward N_2 formation from 60 to 80% (Figure 2). This quantity is determined by the competition between the following reactions that occur on the Pt surface.



The observed increase in selectivity is a consequence of the Na-induced decrease and increase, respectively, in the amounts of molecularly adsorbed NO and atomic N on the surface, thus favoring the first reaction over the second. Qualitatively similar effects on S_{N_2} have been found for the electrochemically promoted reduction of NO by CO ⁸ and by H_2 ⁶ with the same catalyst system.

The systematic effect of V_{WR} on the reaction kinetics (Figures 3 and 4) is also understandable in terms of the effects of the Na promoter. For the range of V_{WR} values investigated in Figures 3 and 4 (clean surface, promoted, and further promoted), EP by Na leads to activity enhancement under all conditions of partial pressure. This is consistent with the arguments developed above. The systematic shift of $P^*_{C_3H_6}$ to higher propene partial pressures (Figure 3) as the sodium coverage is increased reflects an increase in chemisorption bond strength of NO relative to propene with increasing Na coverage. Such behavior is exactly what one would expect in the case of an electropositive promoter: the chemisorption strength of electron donors (propene) should be decreased, whereas the chemisorption of electron acceptors (NO and its dissociation products) should be enhanced.

The systematic increase in activation energies with increasing Na loading deserves some comment. In our earlier EP studies of the $CO + O_2$ ⁵ and $CO + NO$ ⁸ reactions over Pt/ β'' -alumina, a pronounced step increase in E_a was observed as the amount

of Na increased. There is persuasive evidence⁵ that this step change is associated with a surface phase transition—the formation or disruption of islands of CO. Although CO has been detected as a surface intermediate in the Pt-catalyzed oxidation of ethylene,¹³ one may speculate that the absence of a step change in the present case is not unexpected, given the greater chemical complexity of the adsorbed phase. It is possible that the systematically increasing E_a values are at least partly associated with Na-induced increase in chemisorption strength of the three electron-withdrawing adsorbates (Na_a , O_a , NO_a), though the complexity of the system precludes detailed analysis. The increase in E_a s is accompanied by large increases in the preexponential factors (thus giving the net rate acceleration) which may plausibly be associated at least in part with an increased density of sites for NO dissociation due to the presence of Na.

The strong poisoning behavior observed at high Na loadings is understandable in terms of the XPS results (see below) which indicate the presence of large amounts of Na compounds at very negative catalyst potentials. In other words, coverage of active Pt sites by overloading with promoter is a likely major cause of poisoning. Additionally, as noted above, the chemisorption bonds of propene and oxygen should be respectively weakened and strengthened by an electropositive promoter. Therefore, at high levels of Na the coverage of propene should be markedly attenuated, while the activation energy for reactions involving O_a could be increased.

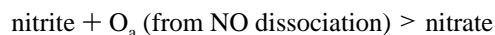
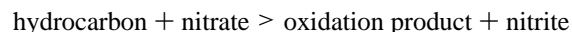
The central assumption underlying all of the preceding discussion is that, under EP conditions, reversible changes in V_{WR} correspond to the reversible pumping of Na to/from the Pt from/to the solid electrolyte. Our XPS data (Figure 6a) clearly demonstrate that such reversible transport of Na between β'' -alumina and the gas-exposed surface of the Pt film does indeed occur under the conditions of voltage and temperature that were used for the reactor studies. This is an important observation that substantiates our view of the mode of action of the EP system. Additionally, the identical electrotransport properties and electron binding energies exhibited by vacuum deposited Na and by electropumped Na in vacuum clearly establish that these are the same chemical species. This is an important point and should help to clarify apparent misunderstandings that sometimes arise about the chemical nature of alkali promoters on metal catalyst surfaces. The mode of delivery of pure Na to the Pt surface is irrelevant: in vacuum it is present as an adatom that has undergone significant charge transfer to the (in this case) Pt surface, $\text{Na}^{\delta+}/\text{Pt}^{\delta-}$. The presence of a reactive gas atmosphere converts this Na into surface compound(s) whose composition and degree of dispersion depend on the temperature and the composition of the gas phase, as discussed below. We have found that these surface compounds can also be electrochemically destroyed by pumping Na away from the Pt film.

The XPS results reveal the identity of the principal surface chemical compounds formed during Na electropumping in the reaction gas. It seems clear that both NaNO_2 and NaNO_3 are formed, and we accordingly identify nitrite and nitrate as the main counterions which, with Na, constitute the promoter phase. This identification depends on the observed N 1s binding energies and the relative tendencies toward wetting and decomposition exhibited by the two nitroxy compounds: the nitrate is *more* thermally stable than the nitrite (Figure 8A). The assignment is strengthened by the observed differences in reactivity towards propene: the nitrate is *more* chemically reactive than the nitrite (Figure 8B). This is also consistent with the observation (Figure 7A) that only nitrite survives to

be detected after withdrawal of a poisoned catalyst from the NO + propene mixture. In this case, the nitrate was reacted away before XP analysis was possible. With the promoted sample, on which both compounds are present in much smaller amounts, neither is detectable after transfer from the reaction mixture. The Na 1s results (Figure 7b) confirm that the poisoned surface is more heavily loaded with Na compounds than the promoted surface; however, the effect is more apparent in the Na *KLL* Auger spectra shown in Figure 7c. This reflects the very different sampling depth in the two cases (electron kinetic energies ~ 180 and ~ 990 eV, respectively). The conclusion is that in the poisoned case the Na compounds are present as very substantial 3D crystallites—this “bulk” material, which presumably covers most of the Pt surface, would contribute significantly to the total intensity of the *KLL* Auger spectrum but would contribute to the Na 1s intensity far less.

The C 1s spectra (Figure 7d) show relatively little carbon retention on the poisoned surface, presumably due to extensive coverage by sodium nitrite/sodium nitrate. The electrochemically cleaned surface accumulated some graphitic carbon, and on the promoted surface the 286.2 eV BE emission indicates the presence of CH_x species;^{21a}—presumably resulting from dissociation and partial oxidation of propene on the promoter-activated surface. Figure 7e shows that the poisoned surface exhibits O 1s emission at 531 and 535 eV BE. The latter is due to the nitrate species;^{21b} the associated emission is quenched by standing in ambient vacuum for 10 h, in line with the behavior of the corresponding N 1s emission (Figure 7a). The origin of the 531 eV BE signal is less clear—given the state of the surface and the sample handling procedures, it is unlikely to be due to O_a on Pt. It could possibly be due to oxidic oxygen associated with Na, although on the basis of the present results we cannot be sure about this. As noted in the Results section, Figures 8a,b nicely shows the different thermal stabilities and reducibilities of the nitrate and nitrite species. These are in accord with the corresponding properties of the bulk materials and the detectable redispersion of the nitrite at 520 K suggest that the nitrite phase might be very mobile at reaction temperature. The O 1s results in Figure 8c confirm that the nitrite and nitrate are reduced by propene. The 532 eV peak corresponds to that also observed in the postreaction experiments (Figure 7e), tentatively assigned above to “oxidic” oxygen; clearly, it is much more resistant to reduction than the nitrate and nitrite. The 533 eV BE shoulder observed in spectrum 4 after the largest dose of propene could be assigned to carbonate; some support for this suggestion comes from the recent observation that CO_a is observed as a surface intermediate during the oxidation of ethylene on Na-promoted Pt{111}.

Finally, we draw attention to an interesting question. The observation that the surface nitrate is efficiently reduced by propene raises the possibility that $\text{NO}_3^-/\text{NO}_2^-$ may constitute a redox couple that is involved in the catalytic turnover, thus



If this were the case, it would mean that we are dealing with a promoter system in which the cation triggers the primary chemistry while the anion facilitates subsequent oxidative reactions. Further work is in progress to investigate this possibility.

Conclusions

1. The catalytic reduction of NO over Pt by propene exhibits strong electrochemical promotion when Na from β'' -alumina

is pumped to the catalyst surface. The effects are reversible with catalyst potential and rate gains of about an order of magnitude over the clean surface rates can be achieved. At sufficiently high Na loadings the reaction is poisoned.

2. All the data are consistent with Na-induced NO dissociation being the critical reaction-initiating step.

3. The selectivity toward N₂ formation *versus* N₂O production always increases with decreasing catalyst potential (increasing Na coverage): this is understandable in terms of point 2.

4. XPS data confirm that the mode of operation of the electrochemically promoted Pt film does indeed involve reversible pumping of Na to or from Pt from or to the solid electrolyte. Under UHV conditions, this electropumped Na is indistinguishable from Na put down by vacuum deposition.

5. Under reaction conditions the Na promoter is present mainly as a mixture of nitrate and nitrite; it is possible that some form of sodium oxide is also present. The nitrate is thermally more stable but also more easily reduced than the nitrite. The loading of promoter compounds is relatively low under promoted conditions and much higher under poisoned conditions. A substantial fraction of the Na compounds is present as 3D crystallites under all reaction conditions.

Acknowledgment. A.P. holds a Postdoctoral External Fellowship, CONICET. A.P. and R.M.L. acknowledge support by the British Council and Fundación Antorchas. Financial support from the UK Engineering and Physical Sciences Research Council under Grant GR/K45562 is gratefully acknowledged.

References and Notes

- (1) Vayenas, C. G.; Bebelis, S.; Yentekakis, I. V.; Lintz, H.-G. *Catal. Today* **1992**, *11* (3), 303.
- (2) Pliangos, C.; Yentekakis, I. V.; Verykios, X.; Vayenas, C. G. *J. Catal.* **1995**, *154*, 124.

- (3) Bebelis, S.; Vayenas, C. G. *J. Catal.* **1989**, *118*, 125.
- (4) Yentekakis, I. V.; Bebelis, S. *J. Catal.* **1992**, *137*, 278.
- (5) Yentekakis, I. V.; Moggridge, G. D.; Vayenas, C. G.; Lambert, R. M. *J. Catal.* **1994**, *146*, 292.
- (6) Marina, O. A.; Yentekakis, I. V.; Vayenas, C. G.; Palermo, A.; Lambert, R. M. *J. Catal.*, in press.
- (7) Lambert, R. M.; Tikhov, M.; Palermo, A.; Yentekakis, I. V.; Vayenas, C. G. *Ionics* **1995**, *5*, 366.
- (8) Palermo, A.; Lambert, R. M.; Harkness, I. R.; Yentekakis, I. V.; Marina, O.; Vayenas, C. G. *J. Catal.* **1996**, *161*, 471.
- (9) Yentekakis, I. V.; Vayenas, C. G. *J. Catal.* **1994**, *149*, 238.
- (10) Politova, T. I.; Sobyenin, V. A.; Belyaev, V. D. *React. Kinet. Catal. Lett.* **1990**, *41*, 321.
- (11) Taylor, K. C. *Catal. Rev.—Sci. Eng.* **1993**, *35*, 457.
- (12) Yentekakis, I. V.; Neophytides, S.; Vayenas, C. G. *J. Catal.* **1988**, *111*, 152.
- (13) Harkness, I. R.; Hardacre, C.; Lambert, R. M.; Yentekakis, I. V.; Vayenas, C. G. *J. Catal.* **1996**, *160*, 19.
- (14) Harkness, I. R.; Lambert, R. M. *J. Catal.* **1995**, *152*, 211.
- (15) Vayenas, C. G.; Bebelis, S.; Despotopoulou, M. *J. Catal.* **1991**, *128*, 415.
- (16) Vayenas, C. G.; Bebelis, S.; Ladas, S. *Nature* **1990**, *343*, 625.
- (17) Bonzel, H. P.; Pirug, G.; Ritke, C. *Langmuir* **1991**, *7*, 3006.
- (18) Cavalca, C.; Larsen, G.; Vayenas, C. G.; Haller, G. L. *J. Phys. Chem.* **1993**, *97*, 6115.
- (19) Ladas, S.; Kennou, S.; Bebelis, S.; Vayenas, C. G. *J. Phys. Chem.* **1993**, *97*, 8845.
- (20) (a) Folkesson, B. *Acta Chem. Scand.* **1973**, *27*, 287. (b) Fuggle, F. G.; Menzel, D. *Surf. Sci.* **1984**, *79*, 1. (c) Kiskinova, M.; Pirug, G.; Bonzel, H. P. *Surf. Sci.* **1983**, *140*, 1.
- (21) (a) Siegban, K.; Nordling, C.; Fahlman, A.; Nordberg, R.; Hamrin, K.; Hedman, J.; Johansson, G.; Bergmark, T.; Karlsson, S.-E.; Lindgren, I.; Lindberg, B. *ESCA-atomic, molecular and solid state structure studies by means of electron spectroscopy*; Nova Acta Regiae Societatis Scientiarum Upsaliensis, ser. IV, 1967; Vol. 20. (b) Allen, H. C.; Laux, J. M.; Vogt, R.; Finlayson-Pitts, B. J.; Hemminger, J. C. *J. Phys. Chem.* **1996**, *100*, 6371.
- (22) Masel, R. I. *Catal. Rev.—Sci. Eng.* **1986**, *28* (2,3), 335.
- (23) Lang, N. D.; Holloway, S.; Norskov, J. K. *Surf. Sci.* **1985**, *150*, 24.
- (24) Harkness, I. R.; Lambert, R. M. *J. Chem. Soc., Faraday Trans.*, in press.